

# New Kinetic Model for Resist Dissolution

Chris A. Mack

SEMATECH, Austin, Texas 78741

## ABSTRACT

A new, enhanced kinetic model for the dissolution rate of photoresists is proposed which builds on the original kinetic model proposed by the author. The new mechanism more accurately describes the chemistry of the dissolution process by taking into account both the dissolution inhibition and the dissolution enhancement effects of a photoactive compound on the base resin. Results are shown which agree with previously published experimental data.

Process models are useful on many different levels. If a model accurately describes the behavior of a physical process, it can be used to quantitatively explore the behavior of the process, the interactions of input variables, and process sensitivities. In addition, if the model has its basis in the fundamental physics or chemistry of the process, it can be useful in understanding the effects of that physics or chemistry.

Simulation of the optical microlithography process used in the fabrication of semiconductor integrated circuits began in the mid 1970s (1, 2), and has progressed greatly since then (3, 4). One important part of every lithography model is a description of the development process. In particular, a development model must predict the development rate of a photoresist as a function of the chemical composition of the resist. (The chemical composition of the resist is intentionally modified by selective exposure of the photoresist to light.) The original Dill development rate model (2) was an empirical curve fit of experimental development rate data. The three parameters for the model had no physical significance and the model fit the data only over a limited range. The Kim model (5) was proposed to improve the fit over the full range of data. The model was again empirical, but at least one of the three parameters had some physical significance. The author proposed a kinetic model for development (6) which will be described in some detail below. This four parameter model is based on a proposed chemical mechanism for the effects of the various chemical species on the development rate. The advantage of the kinetic model is that all of the parameters have physical significance and thus the lithographic behavior of the photoresist can be correlated with the chemical mechanism giving rise to that behavior. Daniels and Trefonas (7) later proposed a similar mechanism for the development rate and gave an explanation as to why this mechanism was reasonable. Shortly thereafter, Hirai (8) proposed the same development rate model.

This paper will propose a new, enhanced kinetic model for development which builds on the original Mack model. The new mechanism more accurately describes the chemistry of the dissolution process.

## Background

A typical diazonaphthoquinone (DNQ) positive photoresist has two basic components. The bulk of the photoresist (typically 70% by weight) is made up of a Novolac resin. By itself, the resin is moderately soluble in the aqueous base used as a developer. The remaining portion of the resist is a photoactive compound (PAC). A PAC will contain one or more photoreactive sites per molecule. Upon exposure to light, the photoactive compound is transformed into a carboxylic acid. The PAC acts to inhibit dissolution of the resin. On the other hand, the carboxylic acid enhances the dissolution of the resist. Thus, exposure results in a solubility change.

The original Mack kinetic model for resist dissolution centered around the principle of dissolution enhancement. A mixture of resin and photoactive compound is considered insoluble. By converting some of the PAC to a carboxylic acid, the dissolution rate is enhanced. Thus, the rate of dissolution is given by

$$R = k_{dev} P^n \quad [1]$$

where  $P$  is the concentration of the carboxylic acid,  $k_{dev}$  is a rate constant, and  $n$  is the order of the reaction. Letting  $M$  be the concentration of PAC reactive sites after the exposure and  $M_0$  the initial concentration, stoichiometry gives

$$P = M_0 - M \quad [2]$$

It is common to normalize the concentrations to  $M_0$  giving

$$p = \frac{P}{M_0}, m = \frac{M}{M_0} \quad [3]$$

Now Eq. [1] can be slightly rearranged to yield

$$R = R_{max} (1 - m)^n \quad [4]$$

where  $R_{max}$ , the maximum dissolution rate, occurs when  $m = 0$  (i.e., after complete exposure) and is given by

$$R_{max} = k_{dev} M_0^n \quad [5]$$

Equation [4] can be modified to take into account the dissolution of unexposed resist by simply adding  $R_{min}$

$$R = R_{max} (1 - m)^n + R_{min} \quad [6]$$

In effect, adding  $R_{min}$  assumes that the dissolution of the unexposed resist occurs by a different, independent mechanism than the dissolution of exposed resist.

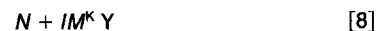
## New Kinetic Model

The previous kinetic model is based on the principle of dissolution enhancement. The carboxylic acid enhances the dissolution rate of the resin/PAC mixture. In reality this is a simplification. There are really two mechanisms at work. The PAC acts to inhibit dissolution of the resin while the acid acts to enhance dissolution. Thus, the rate expression should reflect both of these mechanisms. The following paragraphs present a new proposed mechanism for resist dissolution.

The Novolac resin molecule can undergo two reactions. In the presence of developer, Novolac and carboxylic acid will form a soluble species  $X$  which is dissolved away. For a Novolac concentration of  $N$ , this step gives an elementary reaction



where  $n$  is the number of exposed PAC sites which act in concert to cause dissolution and  $k$  is the rate constant. Novolac can also react with unexposed PAC sites to form an insoluble complex  $Y$ . The resulting reversible reaction, which takes place prior to the development step, is



where  $l$  is the number of unexposed PAC sites which act in concert to form the complex  $Y$ .  $K$  is the equilibrium rate constant and is given by

$$K = \frac{Y}{NM^l} \quad [9]$$

The concentration of available Novolac sites is equal to the ini-

tial Novolac concentration  $N_0$  minus the amount consumed by reaction [8]

$$N = N_0 \cdot Y \quad [10]$$

Combining Eq. [9] and [10] gives

$$N = \frac{N_0}{1 + KM^l} \quad [11]$$

The rate expression resulting from Eq. [8] is

$$\frac{dX}{dt} = kNP^n \quad [12]$$

Using Eq. [11] for the available Novolac concentration gives

$$\frac{dX}{dt} = \frac{kN_0P^n}{1 + KM^l} \quad [13]$$

Dissolution of the photoresist can take place by two methods. The activated resin complex X will dissolve at a rate proportional to  $dX/dt$ . Any Novolac which has not formed the Y complex will dissolve at a rate given by

$$R_{\text{Novolac}} = k'N = \frac{k'N_0}{1 + KM^l} \quad [14]$$

The total dissolution rate  $R$  is the sum of the two rates discussed above

$$R = k'N + k'' \frac{dX}{dt} \quad [15]$$

Combining Eq. [13]-[15] and simplifying the resulting constants gives the desired form of the overall photoresist dissolution rate

$$R = R_{\text{resin}} \frac{1 + k_{\text{enh}}(1-m)^n}{1 + k_{\text{inh}}(m)^l} \quad [16]$$

where  $k_{\text{enh}}$  is a constant representing the enhancement mechanism,  $n$  is the enhancement reaction order,  $k_{\text{inh}}$  is a constant for the inhibition mechanism,  $l$  is the inhibition reaction order, and  $R_{\text{resin}}$  is the development rate of the resin alone ( $= k'N_0$ ).

For no exposure,  $m = 1$  and the development rate is at its minimum. From Eq. [16]

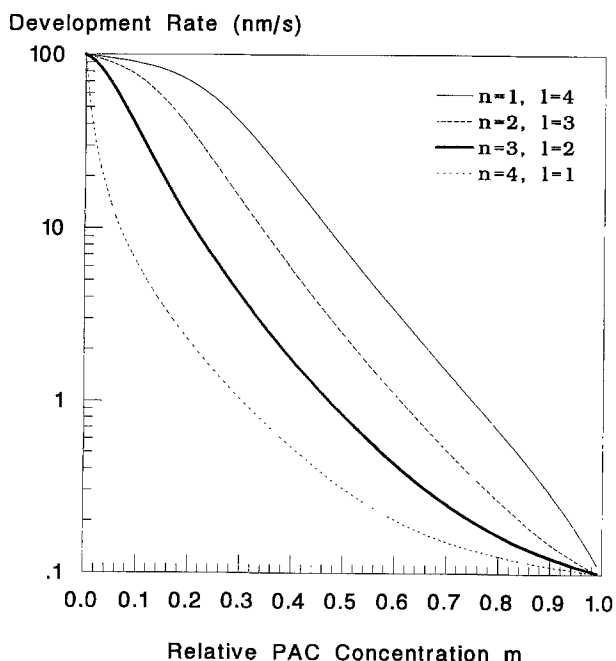


Fig. 1. The enhanced kinetic model for development rate for various values of  $n$  and  $l$  ( $R_{\text{max}} = 100$  nm/s,  $R_{\text{min}} = 0.1$  nm/s,  $R_{\text{resin}} = 10$  nm/s).

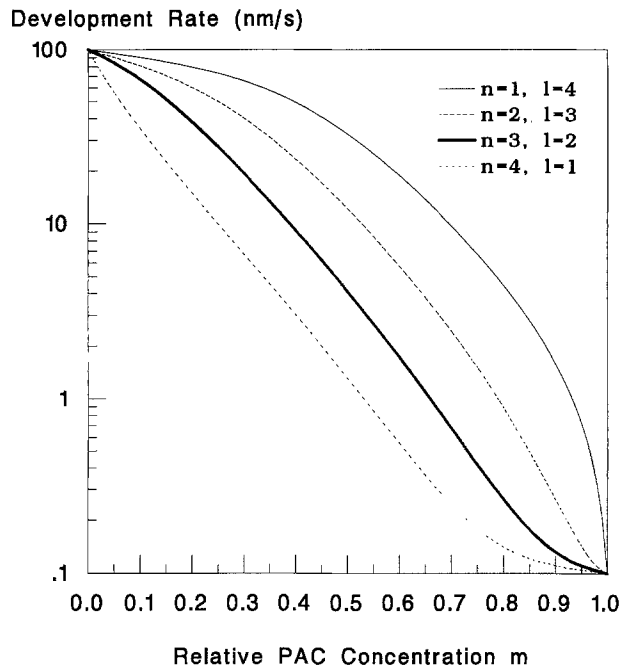


Fig. 2. The enhanced kinetic model for development rate for various values of  $n$  and  $l$  ( $R_{\text{max}} = 100$  nm/s,  $R_{\text{min}} = 0.1$  nm/s,  $R_{\text{resin}} = 1$  nm/s).

$$R_{\text{min}} = \frac{R_{\text{resin}}}{1 + k_{\text{inh}}} \quad [17]$$

Similarly, when  $m = 0$ , corresponding to complete exposure, the development is at its maximum

$$R_{\text{max}} = R_{\text{resin}}(1 + k_{\text{enh}}) \quad [18]$$

Thus, the development rate expression can be characterized by five parameters:  $R_{\text{max}}$ ,  $R_{\text{min}}$ ,  $R_{\text{resin}}$ ,  $n$ , and  $l$ .

Obviously, the enhanced kinetic model for resist dissolution is a superset of the original kinetic model. If the inhibition mechanism is not important, then  $k_{\text{inh}} = 0$ . For this case Eq. [16] is identical to Eq. [6] when

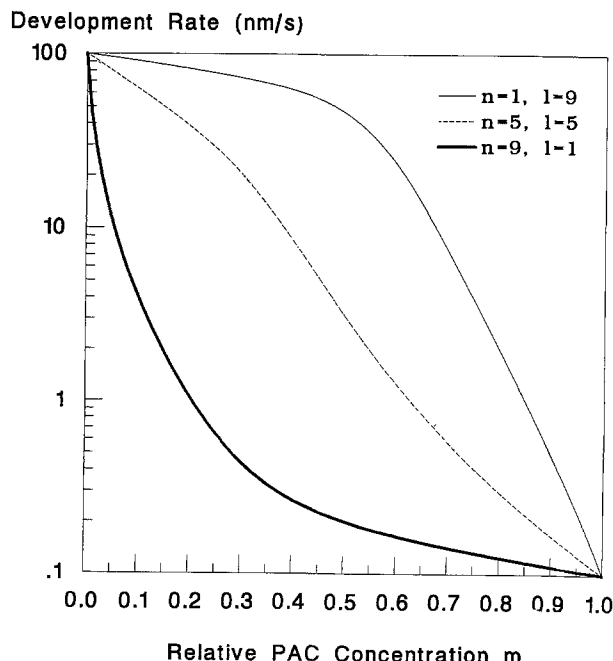


Fig. 3. The enhanced kinetic model for development rate for various values of  $n$  and  $l$  ( $R_{\text{max}} = 100$  nm/s,  $R_{\text{min}} = 0.1$  nm/s,  $R_{\text{resin}} = 10$  nm/s).

$$R_{\min} = R_{\text{resin}}, R_{\max} = R_{\text{resin}} k_{\text{enh}} \quad [19]$$

Figures 1-3 show plots of the enhanced kinetic dissolution model for different values of  $n$ ,  $l$ , and  $R_{\text{resin}}$ . These curves show a variety of different shapes, similar to the shapes found for actual photoresists (9).

The author's original kinetic model also included effects of developer diffusion to the resist surface (6). This diffusion effect can be included with the enhanced kinetic model proposed here in the same way.

### Conclusions

A new model for resist dissolution has been given based on a proposed dissolution mechanism. Each term in the model has physical significance. Thus, by fitting the model to experimental data, one can learn about the chemical kinetics of the dissolution process (e.g., the relative importance of the dissolution enhancement and inhibition mechanisms). Work is now ongoing to compare the predictions of the enhanced kinetic model with experimental results for real and model photoresist systems. Incorporation of this model into a complete lithography simulator will enable lithographers to evaluate the trade-offs between enhancement and inhibition and their effects on resolution and process latitude. Further, photoresist manufacturers may be able to optimize their designs in the same way.

Manuscript submitted Sept. 9, 1991; revised manuscript received Jan. 28, 1992.

SEMATECH assisted in meeting the publication costs of this article.

### REFERENCES

1. F. H. Dill, *IEEE Trans. Electron Dev.*, **ED-22**, 440 (1975).
2. F. H. Dill et al., *ibid.*, **ED-22**, 445 (1975); *Kodak Microelec. Seminar Interface '74*, pp. 44-54 (1974).
3. W. G. Oldham, S. N. Nandgaonkar, A. R. Neureuther, and M. O'Toole, *IEEE Trans. Electron Dev.*, **ED-26**, 717 (1979).
4. C. A. Mack, *Optical Microlith. IV, Proc.*, SPIE Vol. 538, pp. 207-220 (1985).
5. D. J. Kim, W. G. Oldham, and A. R. Neureuther, *IEEE Trans. Electron Dev.*, **ED-31**, 1730 (1984).
6. C. A. Mack, *This Journal*, **134**, 148 (1987).
7. P. Trefonas and B. K. Daniels, *Advances in Resist Technology and Processing IV, Proc.*, SPIE Vol. 771, pp. 194-210 (1987).
8. Y. Hirai et al. *IEEE Trans. Computer Aided Design*, **CAD-6**, 403 (1987).
9. S. G. Hansen et al., *Optical/Laser Microlith. IV, Proc.*, SPIE Vol. 1463, pp. 230-244 (1991).

# On the Texture of Electroless Copper Films on Epitaxial Cu Seed Layers Grown on Si (100) and Si (111) Substrates

Jian Li

Department of Materials Science and Engineering, Cornell University, Ithaca, New York 14853

Y. Shacham-Diamand

School of Electrical Engineering, Cornell University, Ithaca, New York 14853

### ABSTRACT

The orientation control of electroless copper films on copper seed layers with different preferential orientations was investigated. Copper films, deposited by electron-beam evaporation, show an epitaxial relationship with the Si substrates, resulting in (100)- and (111)-oriented Cu films on (100) and (111) Si substrates, respectively. Ion-channeling, plan-view and cross-sectional transmission electron microscopy and x-ray diffraction have been employed to investigate the orientation dependence of the copper layers on the copper seed layers with (100) and (111) orientations and surface condition between electroless copper and E-beam copper layers.

Very recently, interest in copper as an interconnect (1) has generated the need for understanding the oxidation of copper and its alloy films. Copper is readily oxidized at low temperatures (2). Unlike the oxidation of aluminum, the oxidation rate of copper is fast, and no self-protective oxide layer forms to prevent further oxidation. The formation of  $\text{Cu}_2\text{O}$  and  $\text{CuO}$  degrade the electrical and mechanical properties of the copper. Preferential oxidation in some planes of copper was found in the decreasing order of (100), (111), and (110) faces (3). Here, (100) face has the fastest oxidation rate. This suggests that copper films with highly (111) textured grains are more oxidation resistant than those with (100)-texture.

As a potential candidate for ULSI interconnect application, electroless copper deposition is able to produce layers of homogeneous thickness both as surface circuitry and as conductive walls in through-holes of high-aspect ratio (4). It is known that electroless copper films are (111)-oriented at low overpotential and (100)-oriented at medium overpotential (5). Junginger et al. found that the electroless copper films on Ti-seeded glass substrates are (100)-textured when the baths contain surfactant, and (111)-textured when they are free of surfactant (6).

In order to obtain highly textured electroless copper films with high oxidation resistance, a seed layer with controllable

orientation is needed. Chang (8) reported that copper films, deposited by electron-beam evaporation at room temperature without intentional heating of the substrates, show an epitaxial relation with the Si substrates, resulting in (100)- and (111)-oriented copper films on the (100) and (111) Si, respectively. In this paper, we deposited copper by electroless plating on the copper seed layers with (100) or (111) orientations. We investigate the role of surface cleaning of copper seed layers on the texture of electroless deposited copper films.

Copper seed layers were deposited on (100) and (111) Si by using electron beam evaporation. The base pressure of chamber is  $1 \times 10^{-7}$  Torr, and a deposition rate of 0.5 nm/s was used. Si wafers were etched in buffered HF and rinsed in DI water before loading to evaporation chamber. No intentional heating of substrate was made during deposition. The thickness of copper films ranges from 80 nm to 2  $\mu\text{m}$ . Cu electroless plating was made in aqueous solutions. The solutions contain 0.1M  $\text{CuSO}_4$  hydrate, NaOH,  $5 \times 10^{-4}$  M formaldehyde 37% in water,  $\text{CN}^-$ , 0.12M ethylene diamine tetra-acetic acid (EDTA), and surfactants. The sodium hydroxide should be added until the solution pH at room temperature reaches 12.5. The NaOH was added before the cyanide. The Cu was deposited at 60°C with a redox potential of -780 mV. The electroless deposited copper is around 500 nm thick. The overall reaction takes